Line Width Distributions in Single-Molecule Spectroscopy Due to Optical Saturation

L. Kador

University of Bayreuth, Institute of Physics, and "Bayreuther Institut für Makromolekülforschung (BIMF)", D-95440 Bayreuth, Germany

Received: March 4, 1998

The paper deals with distributions of spectroscopic line widths of single molecules as measured in disordered solids at low temperatures. The influence of the random orientation of the dye molecules and, hence, of the different amount of power broadening on the fluorescence excitation spectra is investigated. The resulting line width distributions are calculated as a function of laser intensity and of the detection efficiency of the apparatus. It turns out that, for linearly polarized laser light, power broadening tends to give rise to asymmetric distributions that have a steep slope at narrow widths and a longer tail at broad widths. Possible implications for experimental line width histograms are discussed.

1. Introduction

The spectroscopy of individual molecules in solids at low temperature is a powerful technique that completely avoids any kind of ensemble averaging. Therefore, besides eliminating the ubiquitous phenomenon of inhomogeneous broadening, it yields the possibility to study dye−matrix interactions on a truly local scale and to compare the relevant physical parameters of different single-molecule spectra in the same sample. An overview of this field is provided by several recent reviews.[1−4]

One of the most surprising results of single-molecule spectroscopy was the finding that several (or perhaps most) photophysical parameters of an ensemble of dye molecules in a solid are subject to distributions. This is not only true for the solvent shift of the absorption lines (which leads to inhomogeneous broadening) and for the line shift due to external pressure[5,6] and electric fields,[7] but also the stability with respect to light-induced frequency jumps and the (quasi-)homogeneous line width can be very different for different molecules, in particular in disordered and polycrystalline systems. Even parameters that are usually considered to be of mainly intramolecular nature, such as the triplet population and depopulation rate, can show variations.[8] A distribution of the probability of photophysical transformations opens up the possibility of observing hole-burning spectra and single-molecule lines in the same dye−matrix systems[9] or even in the same samples.[10,11]

An intriguing point is the distribution of single-molecule line widths that was observed in a variety of polymeric[9,12−14] and also crystalline (mainly Sh'polskĭi)[9,15,16] dye−matrix systems. In all cases, the distributions are distinctly asymmetric with a steep rise at narrow widths and a longer tail at broad widths. With the exception of some polymeric systems,[9] the lower cutoff value was mostly found to be close to the lifetime limit of the respective dye molecules.

A possible origin of the line width distributions may be that the dye molecules experience different magnitudes of spectral diffusion.[13] This interpretation is reasonable, since the tunneling systems (TLS's) responsible for the optical frequency jumps are quite dilute, even in completely amorphous polymers,[17] so that the distances to the nearest TLS's can vary from molecule to molecule. The authors of ref 13 were able to describe their line width data with a statistical theory which, in similar form, is also used to model inhomogeneous absorption lines.[18] Apart from spectral diffusion, also differences in fast dephasing (T_2 processes) may lead to line width distributions. The contributions of dephasing (processes faster than the excited-state lifetime T_1) and spectral diffusion (processes slower than T_1) to the line width of a single molecule can, in principle, be determined by measuring the line width and the signal amplitude at different laser intensities.[19] Such power-broadening experiments and the comparison with photon echo data had the result that, at least in some systems, both line width components are indeed subject to distributions.[20]

In disordered solids, there is a third possible origin of line width variations. Since the dye molecules are oriented randomly, the projection of their transition dipole moment on the polarization axis of the laser and, hence, the Rabi frequency and the amount of power broadening will be different. Similar arguments apply also to birefringent crystalline samples in which the polarization state of the laser light changes with depth.[21] To record single-molecule signals with favorable signal-to-noise ratio, the power densities used are often close to the saturation intensity[22] so that power broadening can play a role for part of the molecules (unless the intensity dependence of the line width is measured for each molecule). The purpose of the present paper is to investigate the influence of this effect on the histograms of single-molecule line widths (sections 2.1 and 2.2). It will also be shown how the experimental distribution changes as a function of the fluorescence detection efficiency of the apparatus (section 2.3).

2. Power Broadening of Statistically Oriented Molecules

2.1. Basic Concepts. Let us consider a disordered or polycrystalline solid in which dye molecules are embedded at low concentration. Macroscopically, the orientation of the molecules is random. For a specific molecule, the intensity-dependent zero-phonon line width of an optical transition is given by[22,23]

$$\gamma(\theta) = \gamma_0\sqrt{1 + \frac{I}{I_s}\cos^2\theta} \qquad (1)$$

$\gamma_0 = (\pi T_2)^{-1}$ (in ω units) is the line width in the low-power

10.1021/jp981372l CCC: $15.00
Published on Web 11/03/1998

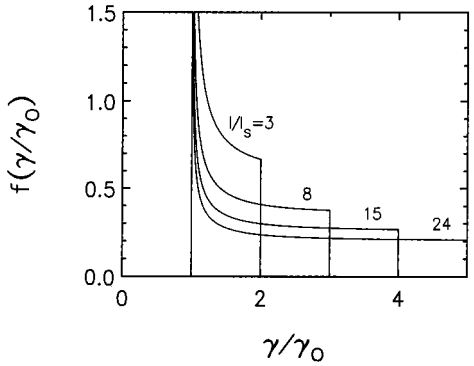

Figure 1. Distribution of the power broadening factor of single-molecule line widths in a disordered system for different laser intensities (eq 3).

limit, I the laser intensity at the position of the molecule, and I_s the saturation intensity, which depends on the intramolecular relaxation rates and is proportional to γ_0.[22] The factor $\cos^2\theta$ accounts for the (squared) projection of the electronic transition dipole moment on the electric-field vector of the laser light, which is assumed to be linearly polarized. Equation 1 describes the simplest case that the molecular lines are not affected by spectral diffusion. The inclusion of spectral-diffusion processes would be straightforward.[19,20]

If the orientation of the molecules is statistical, their relative number at the polar angle θ is given by

$$f(\theta)\,\mathrm{d}\theta = {}^1/_2 \sin\theta\,\mathrm{d}\theta \tag{2}$$

for θ between 0 and π. Using eq 1, this angular distribution can be transformed into a distribution of power-broadened line widths yielding

$$f\left(\frac{\gamma}{\gamma_0}\right) = \left(\frac{I}{I_s}\right)^{-1/2} \frac{\gamma/\gamma_0}{\sqrt{(\gamma/\gamma_0)^2 - 1}} \tag{3}$$

$f(\gamma/\gamma_0)$ is plotted in Figure 1 for some values of the reduced intensity I/I_s. The distribution is defined between the limits $\gamma/\gamma_0 = 1$ (corresponding to $\theta \rightarrow \pi/2$) and $\gamma/\gamma_0 = (1 + I/I_s)^{1/2}$ (corresponding to $\theta \rightarrow 0$ and $\theta \rightarrow \pi$). It has a divergence at its lower bound, yet the integrated area is unity.

The experimental histograms of single-molecule line widths[9,13−16] have shapes that are different from the profiles in Figure 1. This shows that the simple orientational effect cannot be the main origin of the line width variations. One has to bear in mind, however, that the divergence of the theoretical distribution at its lower bound corresponds to those molecules whose transition dipoles are oriented almost perpendicularly to the laser field ($\theta \approx \pi/2$) and which yield, therefore, very weak signals and are difficult to detect. Hence, the divergence will not be observable in experiment. We will come back to this point in section 2.3.

2.2. Distribution of Single-Molecule Line Widths. In this section we consider a distribution of single-molecule line widths γ_0 and investigate its apparent alteration due to the random molecular orientation and the different amount of power broadening. Again, spectral diffusion is not taken into account. As was mentioned above, the saturation intensity I_s is proportional to γ_0. The proportionality constant, which depends on molecular parameters, will be set equal to one in the following so that $I_s = \gamma_0$. The actual laser intensity I must then be properly rescaled (see below). If there is a distribution $p(\gamma_0)$ of "true" line widths, the resulting experimental distribution is obtained

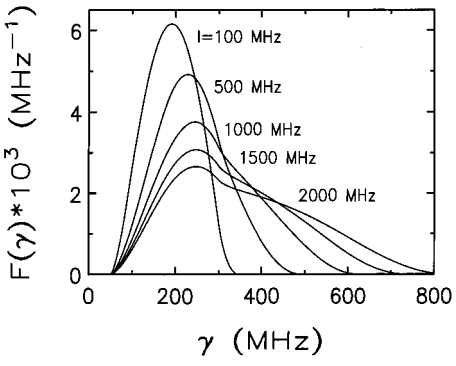

Figure 2. Distribution of power-broadened single-molecule line widths γ (eq 6) for a γ_0 distribution according to eq 7 and different laser intensities I.

by transforming eq 3 into a distribution of absolute line widths and integrating over γ_0

$$F(\gamma) = \int_{\gamma_{0,1}}^{\gamma_{0,2}} f(\gamma|\gamma_0)\, p(\gamma_0)\,\mathrm{d}\gamma_0 \tag{4}$$

The upper integration bound corresponds to unbroadened molecules ($\theta \rightarrow \pi/2$) for which $\gamma_0 = \gamma$. The lower bound describes maximal power broadening ($\theta \rightarrow 0$ and $\theta \rightarrow \pi$) according to

$$\gamma_{0,1} = \sqrt{\gamma^2 + \left(\frac{I}{2}\right)^2} - \frac{I}{2} \tag{5}$$

Therefore, the experimental distribution reads

$$F(\gamma) = \frac{\gamma}{\sqrt{I}} \int_{\sqrt{\gamma^2+(I/2)^2}-I/2}^{\gamma} \frac{p(\gamma_0)}{\sqrt{\gamma_0}\sqrt{\gamma^2 - \gamma_0^2}}\,\mathrm{d}\gamma_0 \tag{6}$$

The integral must be calculated numerically. Mathematically, $F(\gamma)$ and $p(\gamma_0)$ are not related by a convolution. Therefore, it is not possible to perform a deconvolution, i.e., a general calculation of $p(\gamma_0)$ from the experimental distribution $F(\gamma)$. Figure 2 shows typical shapes of $F(\gamma)$ for a smooth symmetrical γ_0 distribution. For simplicity, the following form was chosen

$$p(\gamma_0) = \begin{cases} \dfrac{\pi}{2(\gamma_0^{\max} - \gamma_0^{\min})} \sin\left(\pi \dfrac{\gamma_0 - \gamma_0^{\min}}{\gamma_0^{\max} - \gamma_0^{\min}}\right) & \text{for } \gamma_0^{\min} \le \gamma_0 \le \gamma_0^{\max} \\ 0 & \text{else} \end{cases} \tag{7}$$

with limits $\gamma_0^{\min} = 50$ MHz and $\gamma_0^{\max} = 300$ MHz which correspond approximately to the data of tetrakis(*tert*-butyl)-terrylene in polyisobutylene.[14] The resulting distribution $F(\gamma)$ is plotted for different laser intensities I (rescaled to frequency units) between 100 and 2000 MHz. In these units, I denotes that intensity which, for a molecular line with $\gamma_0 = I$ and $\theta = 0$, causes power broadening by a factor of $\sqrt{2}$ (see eq 1).

The experimental distribution $F(\gamma)$ broadens and becomes distinctly asymmetric with increasing laser intensity. For intermediate to high intensities, its shape is quite similar to the histograms that were actually measured.[9,13−16] Therefore, if distributions of single-molecule line widths are recorded only at one certain light intensity, it is difficult to decide whether their shape and width are influenced by this effect. In the experimental studies cited above it was checked that the measured histograms were not affected by power broadening.

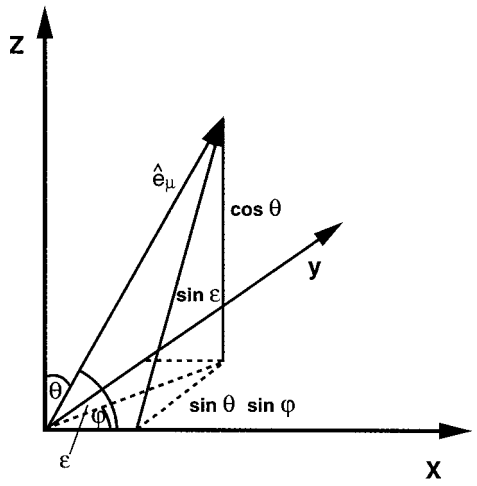

Figure 3. Sketch of the experimental geometry. The laser is polarized in the *z* direction, and the fluorescence photons are detected along the *x* axis.

At higher light intensities, however, an additional asymmetric broadening as shown in Figure 2 would occur.

The profiles in Figure 2 show the strongest possible intensity dependence of $F(\gamma)$ that occurs if there are no spectral-diffusion processes on time scales faster than the measuring time. In the presence of spectral diffusion, the observed power broadening is weaker.[19]

2.3. Influence of Detection Efficiency. The distributions in Figure 2 were calculated under the assumption that all the dye molecules in the sample emit detectable fluorescence signals, even those with θ close to $\pi/2$. In reality, the photon detection efficiency of typical single-molecule experiments is only on the order of 10^{-3},[24] and moreover, there is an unavoidable background level due to scattered light and dark counts. Hence, molecules in a certain angular interval around $\theta = \pi/2$ are invisible. The influence of this effect will be investigated in the following.

The intensity-dependent fluorescence emission rate of a molecule is given by[23]

$$C^*(\theta) = C_\infty \frac{(I/I_s)\cos^2\theta}{1 + (I/I_s)\cos^2\theta} \tag{8}$$

C_∞ being the limiting value for $I \rightarrow \infty$. Setting again $I_s = \gamma_0$ and solving eq 1 for $\cos^2\theta$, we can express the fluorescence emission rate as a function of γ and γ_0

$$C^*(\gamma|\gamma_0) = C_\infty \frac{(\gamma/\gamma_0)^2 - 1}{(\gamma/\gamma_0)^2} \tag{9}$$

The emission pattern of a dipole is proportional to $\sin^2\epsilon$, where ϵ denotes the angle between the axis of the dipole and the emission direction.[24,25] In the following we assume collinear geometry, i.e., the **k** vector of the irradiated laser light and the observation direction are on a straight line. If the aperture of the light-collecting optics is neglected and is assumed to be zero, the detected signal is proportional to

$$C(\gamma|\gamma_0) = C^*(\gamma|\gamma_0)\sin^2\epsilon \tag{10}$$

The opposite limit of very large aperture will be discussed below. From Figure 3 we see that

$$\sin^2\epsilon = \cos^2\theta + \sin^2\theta\sin^2\phi = \cos^2\theta\cos^2\phi + \sin^2\phi \tag{11}$$

ϕ being the azimuthal angle of the transition dipole of a specific dye molecule.

We assume that a molecule can only be detected if its fluorescence count rate C is larger than some lower limit κC_∞ with $0 < \kappa < 1$. For $\kappa \rightarrow 0$ all molecules yield detectable signals, whereas for $\kappa \rightarrow 1$ no molecule is visible. In real experiments, κ can vary over a broad range. For the crystalline system terrylene in *p*-terphenyl, which yields very intense signals,[26] κ would be well below 10^{-3} (the dye molecules are not oriented randomly in this case, however); in polymeric systems with distinctly smaller single-molecule signals,[9] κ is estimated at 0.3 or higher.

Introducing a dimensionless variable $x = \gamma_0/\gamma$ and setting $C(\gamma|\gamma_0) = \kappa C_\infty$, we obtain from eqs 9, 10, and 11

$$x^4\cos^2\phi - x^3\frac{I}{\gamma}\sin^2\phi - x^2\,2\cos^2\phi + x\frac{I}{\gamma}(\sin^2\phi - \kappa) + \cos^2\phi = 0 \tag{12}$$

This fourth-order polynomial in x must be solved numerically for given values of I, γ, κ, and ϕ. It has exactly one real zero in the interval [0, 1]. Denoting this zero by x_0^ϕ and setting $\gamma_{0,2}^\phi = x_0^\phi\gamma$ yields the maximum γ_0 value in the distribution, which, for the parameters given, corresponds to a power-broadened line width of γ and emits a detectable fluorescence signal. For certain combinations of the parameters (e.g., I too low or κ and γ too large), $\gamma_{0,2}^\phi$ may be smaller than the lower integration limit $\gamma_{0,1} = [\gamma^2 + (I/2)^2]^{1/2} - I/2$, in which case no molecules with power-broadened width γ are detectable. Hence, we have

$$F_\phi(\gamma) = \begin{cases} \dfrac{\gamma}{\sqrt{I}}\displaystyle\int_{\sqrt{\gamma^2+(I/2)^2}-I/2}^{\gamma_{0,2}^\phi} \frac{p(\gamma_0)}{\sqrt{\gamma_0}\sqrt{\gamma^2-\gamma_0^2}}\,\mathrm{d}\gamma_0 & \text{for } \sqrt{\gamma^2+(I/2)^2} - I/2 < \gamma_{0,2}^\phi \\ 0 & \text{else} \end{cases} \tag{13}$$

Equation 13 describes the γ distribution if only a subset of molecules with a certain azimuthal orientation ϕ are taken into account. In a disordered solid, all ϕ values occur with equal probability. Therefore, the experimental line width distribution is finally obtained as

$$F(\gamma) = \frac{2}{\pi}\int_0^{\pi/2} F_\phi(\gamma)\,\mathrm{d}\phi \tag{14}$$

Owing to the dependence of eq 12 on $\sin^2\phi$ and $\cos^2\phi$, it is sufficient to consider the interval [0, $\pi/2$].

The above assumption of a vanishingly small aperture of the light-collecting optics is a crude approximation since in single-molecule experiments it is essential to use high-aperture optics for collecting the fluorescence over a solid angle as large as possible. In the ideal case (which is not achieved in reality either), a solid angle of 2π would be covered. In this case the factor $\sin^2\epsilon$ in eq 10 is replaced by unity and the upper integration bound in eq 13 is analytically obtained as $\gamma_{0,2} = \gamma(1-\kappa)^{1/2}$ (independent of ϕ). Hence, averaging over ϕ according to eq 14 is not necessary. In both limiting cases, the upper integration limit tends to γ for $\kappa \rightarrow 0$ and eqs 13 and 14 become identical to eq 6. The area underneath the graph of $F(\gamma)$ is equal to unity for $\kappa = 0$ and decreases with increasing κ.

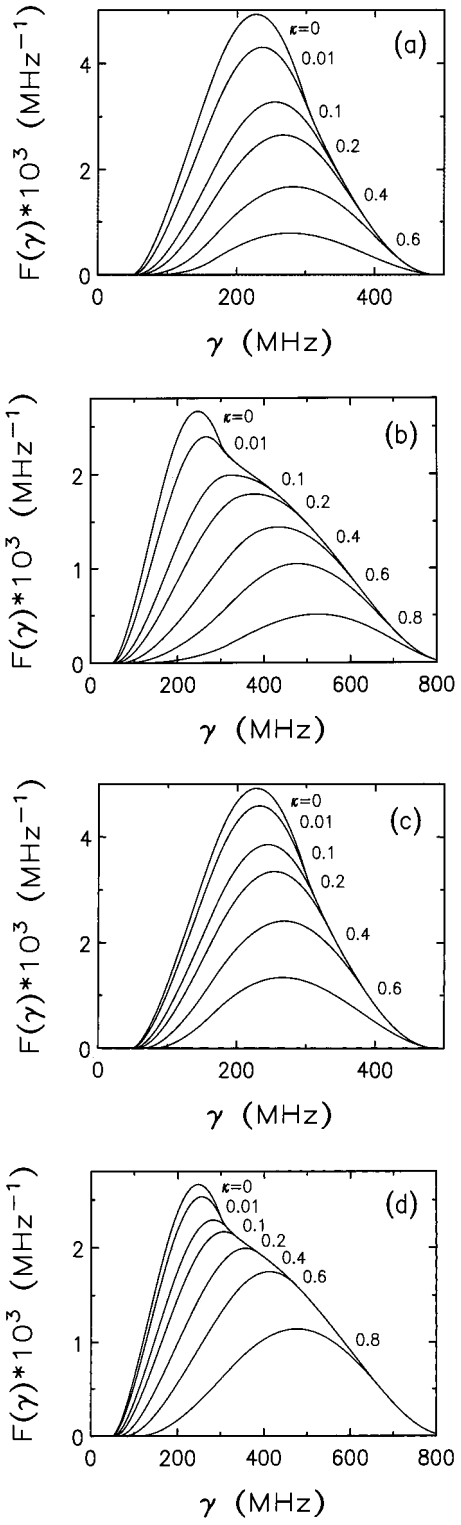

Figure 4. Distribution of detectable single-molecule line widths for different photon detection efficiencies κ and laser intensities I of 500 MHz [(a) and (c)] and 2000 MHz [(b) and (d)]. The distributions in (a) and (b) correspond to vanishingly small aperture of the light-collecting optics, and those in (c) and (d) to a covered solid angle of 2π. Calculation according to eqs 13 and 14.

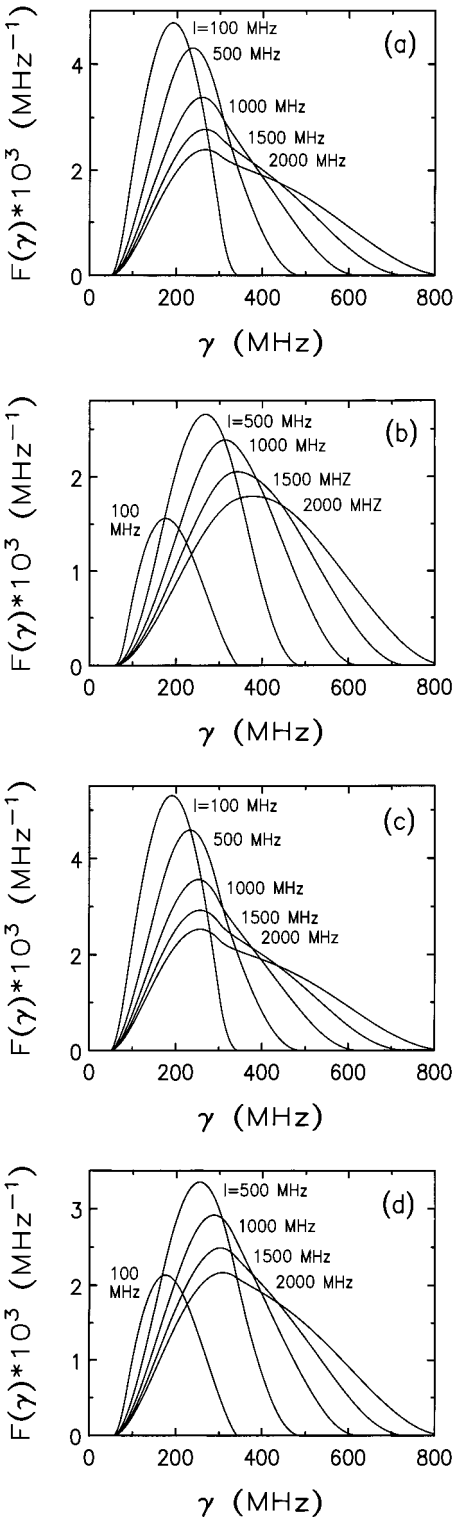

Figure 5. Distribution of detectable single-molecule line widths for different laser intensities I and photon detection efficiencies κ of 0.01 [(a) and (c)] and 0.2 [(b) and (d)]. The distributions in (a) and (b) correspond to vanishingly small aperture of the light-collecting optics, and those in (c) and (d) to a covered solid angle of 2π. Calculation according to eqs 13 and 14.

The shapes of the distribution $F(\gamma)$ are plotted in Figures 4 and 5 for both limiting cases of zero and very large aperture of the optics. Figure 4 shows the profiles for two fixed laser intensities I (Figure 4a,c, 500 MHz; Figure 4b,d, 2000 MHz in the frequency units introduced in section 2.2) and various values of κ. For $p(\gamma_0)$, the form of eq 7 with $\gamma_0^{\min} = 50$ MHz and $\gamma_0^{\max} = 300$ MHz was used again. The general trend for both intensity values is that the maximum of the experimental distribution shifts to broader line widths for decreasing sensitivity of the experiment (i.e., increasing κ), since molecules that experience stronger power broadening emit more intense fluorescence signals and are detected with higher probability.

Only for low laser intensities and large κ, the shift is reversed because in this case the strongest relative power broadening (and, hence, the highest emission rate of fluorescence photons) occurs for molecules at the lower end of the γ_0 distribution. The low laser intensity cannot pump the broader lines at a sufficiently high rate. At both laser intensities, a sizable fraction of the total ensemble of molecules is invisible even for κ as low as 0.1. The reason is that the relative number of molecular orientations scales with $\sin\theta$, which means that there are many molecules with improper orientations relative to the polarization axis of the laser (cf. the divergence in Figure 1 for $\gamma/\gamma_0 \rightarrow 1$). A larger fraction of the dopant molecules in a disordered solid can be detected if unpolarized or circularly polarized laser light is used (see Appendix). The shape of the distributions is not very different for small (Figure 4a,b) and large (Figure 4c,d) apertures of the light-collecting optics. In a real single-molecule experiment, the detection efficiency is usually fixed and only the laser intensity can be easily changed. This is the situation shown in Figure 5 for $\kappa = 0.01$ (parts a and c) and 0.2 (parts b and d). Again both limiting cases of small (parts a and b) and large (parts c and d) apertures are considered. The corresponding profiles for $\kappa = 0$ are plotted in Figure 2. The broadening of the distribution and the shift of its maximum with increasing intensity are obvious. For small detection efficiency, there is also a substantial increase of the area at low intensities (Figure 5b,d). It must again be emphasized that the variation of $F(\gamma)$ will be less pronounced if fast spectral-diffusion processes are present.[19,20]

3. Summary and Conclusions

It was investigated how the different amount of power broadening of randomly oriented dye molecules affects the experimentally observed distributions of single-molecule line widths in disordered solids at low temperatures. If all the molecules have the same (unbroadened) width γ_0, the distribution starts with a divergence at $\gamma = \gamma_0$ and has a sharp cutoff at $\gamma = \gamma_0(1 + I/\gamma_0)^{1/2}$. If there is a γ_0 distribution, the resulting histogram of γ is smooth but asymmetric with a steeper slope at small widths and a longer tail at large widths (for linearly polarized laser light). To decide whether an experimental line width distribution is influenced by power broadening, the experiment must be performed with different light intensities. In this context microscopic techniques[10,27] are particularly promising, since they allow for fast parallel recording of many single-molecule lines so that bleaching or hole-burning effects that are often a problem in disordered systems can be kept small. The orientational disorder is not the only possible origin of a distribution of single-molecule line widths due to optical saturation. The intensity distribution in the laser focus has a similar effect. This point was not addressed in the present paper.

Acknowledgment. The author thanks D. Haarer and A. Müller for many valuable discussions. Financial support of the Deutsche Forschungsgemeinschaft is gratefully acknowledged.

Appendix. Calculation for Unpolarized or Circularly Polarized Light

If the experiment is performed with unpolarized or circularly polarized light, eq 1 is replaced by

$$\gamma(\epsilon) = \gamma_0 \sqrt{1 + \frac{I}{2I_s}\sin^2\epsilon} \qquad \text{(A1)}$$

where ϵ is the angle between the molecular transition dipole and the **k** vector of the laser light (see Figure 3). For one single γ_0, this leads to a line width distribution of

$$f\left(\frac{\gamma}{\gamma_0}\right) = \left(\frac{I}{2I_s}\right)^{-1/2} \frac{\gamma/\gamma_0}{\sqrt{1 + I/(2I_s) - (\gamma/\gamma_0)^2}} \qquad \text{(A2)}$$

which replaces eq 3. It has a divergence at the upper rather than the lower limit. As a consequence, the factor $(\gamma^2 - \gamma_0^2)^{-1/2}$ in eqs 6 and 13 now reads $\{\gamma_0^2[1 + I/(2I_s)] - \gamma^2\}^{-1/2}$ and I is replaced by $I/2$ everywhere.

Assuming collinear detection geometry as above, eq 12 simplifies to

$$x^4 - 2x^2 - x\frac{\kappa I}{2\gamma} + 1 = 0 \qquad \text{(A3)}$$

in the limit of vanishingly small aperture of the light-collecting optics. It has one real zero x_0 in the interval [0, 1]. $\gamma_{0,2} = x_0\gamma$ is the upper integration limit in eq 13. In the opposite case of large-aperture optics, the upper integration bound reads $\gamma_{0,2} = \gamma(1 - \kappa)^{1/2}$ as above. Averaging over ϕ according to eq 14 is not necessary in both cases, and the modified equations 6 and 13 describe the experimental line width distributions for $\kappa = 0$ and $\kappa \neq 0$, respectively.

References and Notes

(1) Moerner, W. E.; Basché, Th. *Angew. Chem.* **1993**, *105*, 537; *Angew. Chem., Int. Ed. Engl.* **1993**, *32*, 457.
(2) Kador, L. *Phys. Stat. Solidi b* **1995**, *189*, 11.
(3) Basché, Th., Moerner, W. E., Orrit, M., Wild, U. P., Eds. *Single-Molecule Optical Detection, Imaging and Spectroscopy*; VCH: Weinheim, 1997.
(4) Plakhotnik, T.; Donley, E. A.; Wild, U. P. *Annu. Rev. Phys. Chem.* **1997**, *48*, 181.
(5) Croci, M.; Müschenborn, H. J.; Güttler, F.; Renn, A.; Wild, U. P. *Chem. Phys. Lett.* **1993**, *212*, 71.
(6) Müller, A.; Richter, W.; Kador, L. *Chem. Phys. Lett.* **1995**, *241*, 547.
(7) Orrit, M.; Bernard, J.; Zumbusch, A.; Personov, R. I. *Chem. Phys. Lett.* **1992**, *196*, 595.
(8) Basché, Th.; Kummer, S.; Bräuchle, C. *Chem. Phys. Lett.* **1994**, *225*, 116.
(9) Kozankiewicz, B.; Bernard, J.; Orrit, M. *J. Chem. Phys.* **1994**, *101*, 9377.
(10) Bach, H.; Irngartinger, Th.; Renn, A.; Wild, U. P. *Mol. Cryst. Liq. Cryst.* **1996**, *291*, 89.
(11) Müller, A.; Richter, W.; Kador, L. *Chem. Phys. Lett.* **1998**, *285*, 92.
(12) Basché, Th.; Ambrose, W. P.; Moerner, W. E. *J. Opt. Soc. Am. B* **1992**, *9*, 829.
(13) Fleury, L.; Zumbusch, A.; Orrit, M.; Brown, R.; Bernard, J. *J. Lumins.* **1993**, *56*, 15.
(14) Tittel, J.; Kettner, R.; Basché, Th.; Bräuchle, C.; Quante, H.; Müllen, K. *J. Lumins.* **1995**, *64*, 1.
(15) Vacha, M.; Liu, Y.; Nakatsuka, H.; Tani, T. *J. Chem. Phys.* **1997**, *106*, 8324.
(16) Vacha, M.; Tani, T. *J. Phys. Chem. A* **1997**, *101*, 5027.
(17) Kador, L. J. *Lumins.* **1993**, *56*, 165.
(18) Stoneham, A. M. *Rev. Mod. Phys.* **1969**, *41*, 82.
(19) Plakhotnik, T. *Opt. Commun.* **1996**, *123*, 105.
(20) Vainer, Yu. G.; Plakhotnik, T. V.; Personov, R. I. *Chem. Phys.* **1996**, *209*, 101.
(21) Güttler, F.; Croci, M.; Renn, A.; Wild, U. P. *Chem. Phys.* **1996**, *211*, 421.
(22) de Vries, H.; Wiersma, D. A. *J. Chem. Phys.* **1980**, *72*, 1851.
(23) Ambrose, W. P.; Basché, Th.; Moerner, W. E. *J. Chem. Phys.* **1991**, *95*, 7150.
(24) Plakhotnik, T.; Moerner, W. E.; Palm, V.; Wild, U. P. *Opt. Commun.* **1995**, *114*, 83.
(25) Jackson, J. D. *Classical Electrodynamics*; Wiley: New York, 1975; p 397.
(26) Kummer, S.; Basché, Th.; Bräuchle, C. *Chem. Phys. Lett.* **1994**, *229*, 309.
(27) Irngartinger, Th.; Renn, A.; Wild, U. P. *J. Lumins.* **1996**, *66* and *67*, 232.